Available online at www.sciencedirect.com
SCIENCE DIRECT®
PERGAMON
Polyhedron 22 (2003) 2077–2090
POLYHEDRON
www.elsevier.com/locate/poly

Theoretical studies of molecule-based magnetic conductors

Kizashi Yamaguchi [a,*], Takashi Kawakami [a], Takeshi Taniguchi [a], Shuhei Nakano [a], Yasutaka Kitagawa [a], Hidemi Nagao [b], Tadafumi Ohsaku [a], Ryo Takeda [a]

[a] *Department of Chemistry, Graduate School of Science, Osaka University, Toyonaka, Osaka 560-0043, Japan*
[b] *Department of Computational Science, Faculty of Science, Kanazawa University, Kakuma, Kanazawa 560-0043, Japan*

Received 6 October 2002; accepted 3 April 2003

Abstract

Our theoretical efforts towards molecule-based magnetic conductors and superconductors on the basis of ab initio Hamiltonians and effective model Hamiltonians are summarized in relation to recently developed π–d systems, for which transition metal complexes have been used as spin sources. Organic π-electron donors or acceptors coupling with organic radicals (R) are also investigated as possible π–R interaction systems. In order to elucidate electronic and magnetic properties of these species, effective exchange integrals (J_{ab}) for magnetic clusters are calculated by ab initio hybrid density functional (HDFT) methods. The ab initio J_{ab} values are numerically reproduced by using model Hamitonians such as $t-J$, Kondo, Anderson and RKKY models. Theoretical possibilities of magnetic conductors and spin-mediated superconductors are elucidated on the basis of these models in the intermediate region for metal–insulator transitions. Interrelationships among magnetism, superconductivity and fluctuations in strongly correlated electron systems are discussed on the basis of the SO(5) and three-dimensional quantum electrodynamics (QED_3) theories. External magnetic field effects such as Jaccarino–Peter effect are also examined for elucidation of magnetic field induced superconductivity. Implications of the calculated results are finally discussed in order to obtain a unified picture of many p–d, π–d and π–R molecule-based systems with strong electron correlations.

Keywords: Magnetic conductors; Magnetic superconductor; π–d; Effective exchange intregal; Hybrid density functional method; Jaccarino–Peter effect

1. Introduction

Past decade, molecule-based materials in intermediate or strong electron correlation regime have attracted much interest in relation to molecular magnetism, magnetic conductivity and superconductivity [1]. Discovery of high-T_c superconductivity of copper oxides urged us to elucidate possible interplay between p- and d-electrons of transition-metal oxides near metal-to-insulator transition [2–4]. Now, it is well established that copper oxides are antiferromagnets before doping, while the species after doping exhibit the high-T_c superconductivity. In a previous paper [5,6], we have examined several model Hamiltonians for copper oxides to elucidate the mechanism of the high-T_c superconductivity: (1) J-model; (2) spin-fluctuation model; (3) spin- and charge-fluctuation model, which is referred to as an electron correlation (EC) model [5]; and (4) charge-fluctuation (CF) or CT model. Now, the models (1–3) are compatible with accumulated experimental results for copper oxides [4]. Recent magnetic field effects on copper oxides [7–9] have revealed the coexistence of d-wave superconductivity (dSC) and antiferromagnetism (AFM) or spin density wave (SDW) states. The SO(5) and three-dimensional quantum electrodynamics (QED_3) theories [10–13] have been developed to obtain a unified description of these states.

Previously [5,6,14–28], we have investigated possible organic, organometallic and inorganic analogs to copper oxides on the basis of the above models (1–4), which permit the nonconventional BCS mechanisms such as

* Corresponding author. Tel.: +81-668-50-5405; fax: +81-668-50-5550.
E-mail address: yama@chem.sci.osaka-u.ac.jp (K. Yamaguchi).

0277-5387/03/$ - see front matter © 2003 Elsevier Science Ltd. All rights reserved.
doi:10.1016/S0277-5387(03)00295-X

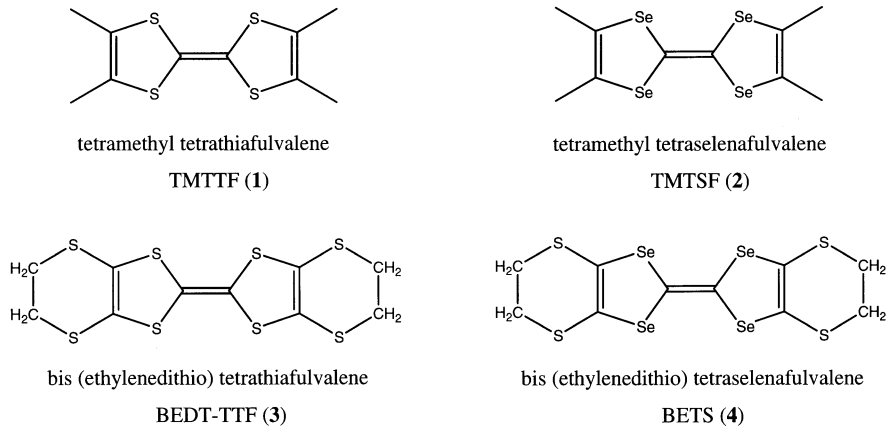

Fig. 1. Molecular structures of TMTTF (**1**), TMTSF(**2**), BEDT-TTF (**3**) and BETS (**4**).

dSC. A crucial role of the electron–phonon (e–p) interaction has been assumed as a common mechanism of the superconductivity of TTF-derivatives such as TMTTF (**1**), TMTSF (**2**), BEDT-TTF (**3**) and BETS (**4**) whose molecular structures are illustrated in Fig. 1. However, recently developed π–d conjugated systems such as κ-(BEDT-TTF)$_2$X (X = Cu(NCN)$_2$ (**5a**), Cu[N(CN)$_2$]Cl (**5b**), Cu[N(CN)$_2$]Br) (**5c**)) exhibited non-BCS behaviors [29–31]. It was also found that the antiferromagnetic (AF) phase exists near the superconducting (SC) one in these organic systems like copper oxides. This may indicate that a common magnetic interaction is operative for π–d, π–R and p–d systems with strong electron correlation [5].

In the present paper, we summarize our basic ideas, strategies and theoretical framework towards molecule-based magnetic conductors [14–28]. To this end, we first perform ab initio calculations of effective exchange integrals (J_{ab}) for TTF-derivatives and related species in order to elucidate magnetic behaviors of the species. The effective Hamiltonians such as Hubbard, Heisenberg, Anderson and Hubbard-Kondo models are used to reproduce ab initio J_{ab} values for these species. Phenomenological models for magnetic, superconductor and other phases are presented by the use of the J_{ab} values. The SO(5) and QED$_3$ theories [10–13] are applied to rationalize these models. External magnetic field effects [32–37] such as Jaccarino–Peter effect [38] are also discussed for elucidation of electronic properties of molecule-based materials near metal (superconductor) to antiferromagnet transition. We also examine previous theoretical models for conducting, magnetic and SC phenomena in relation to recently developed π–d conjugated systems such as κ-(BEDT-TTF)$_2$X, and extend our basic ideas for molecular design of new extended systems. Several theoretical models have been proposed from these investigations for active controls of spin-mediated properties of isoelectronic polymer and other molecule-based systems [14–28].

2. Ab initio computation of effective exchange integrals

2.1. Theoretical models

Band models based on the extended Hückel tight-binding approximation work well for theoretical understanding of many molecular conductors such as TTF-derivatives [39]. However, recent experiments have revealed that AF state appear even in organic systems such as κ-(BEDT-TTF)$_2$X because of strong electron correlation, and resulting Mott insulators usually entail localized spins. Magnetism is also one of key issues in TTF-derivatives with metal complexes and other related species. Their magnetic properties have been investigated by the Heisenberg-type spin coupling Hamiltonian [40–44]

$$H(HB) = -\sum_{ab} 2J_{ab} 2S_a \bullet S_b \qquad (1)$$

where J_{ab} is the orbital-averaged effective exchange integral between the a-th and b-th radical sites with total spin operators S_a and S_b. Recent development of the ab initio computational techniques has made it possible to calculate the J_{ab} values for TTF-derivatives [45]. These methods are classified into two types. One is the spin-symmetry adapted (SA) perturbational and configuration interaction (CI) approach. Use of the SA method is desirable for quantitative computations of J_{ab}, but it is hardly applicable to transition-metal complexes because of high computational costs. The other is the broken-symmetry (BS) approach [40–44], which is often used for such systems because of lower computational costs, though the spin contamination problem occurs in the low-spin (LS) state [43].

Broken-symmetry (BS) calculations of J_{ab} for molecule-based magnets have been performed on the basis of different computational schemes such as Eqs. (2a), (2b) and (2c).

$$J_{ab}^{(1)} = \frac{^{LS}E(X) - {}^{HS}E(X)}{S_{max}^2} \tag{2a}$$

$$J_{ab}^{(2)} = \frac{^{LS}E(X) - {}^{HS}E(X)}{S_{max}(S_{max}+1)} \tag{2b}$$

$$J_{ab}^{(3)} = \frac{^{LS}E(X) - {}^{HS}E(X)}{^{HS}\langle S^2\rangle - {}^{LS}\langle S^2\rangle} \tag{2c}$$

where $^{Y}E(X)$ and $^{Y}\langle S^2\rangle(X)$ denote, respectively, total energy and total spin angular momentum for the spin state Y by the method X (= UHF, UDFT, etc). The first scheme $J_{ab}^{(1)}$ has been derived by Ginsberg [40], Noodleman [41], Noodleman and Davidson [42] (GND), while the second scheme $J_{ab}^{(2)}$ has been proposed by GND, Bencini et al. [44]. $J_{ab}^{(1)}$ is derived when the overlap of magnetic orbitals is sufficiently small, while $J_{ab}^{(2)}$ is applicable when the overlap is sufficiently large. $J_{ab}^{(3)}$ by our approximate spin projection (AP) procedure [43] is close to $J_{ab}^{(1)}$ by GND if $^{HS}\langle S^2\rangle = S_{max}(S_{max}+1)$ and $^{LS}\langle S^2\rangle = S_{max}$, where S_{max} is the spin size for the high-spin (HS) state. $J_{ab}^{(3)}$ becomes equivalent to $J_{ab}^{(2)}$ in the strong overlap region, where $^{LS}\langle S^2\rangle \approx 0$ [43]. Therefore, our scheme [43] involves others [40–42,44] as the strong and weak correlation limits. As shown previously [46], our AP scheme can be extended to trinuclear, and more larger clusters, though $J_{ab}^{(1)}$ and $J_{ab}^{(2)}$ do not work for them. For example, $J_{ab}^{(3)}$ in Eq. (2c) is applicable to linear trinuclear complexes and ring form of tetranuclear complexes [47]. On the other hand, $J_{ab}^{(4)}$ without spin projection is given for both linear and ring forms by:

$$J_{ab}^{(4)} = \frac{^{LS}E(X) - {}^{HS}E(X)}{4(N-1)S_aS_b} \tag{3}$$

where N is the total spin site number and S_c is the size of spin S_c (c = a, b). This equation is applicable to periodic systems involving the same cluster unit cells [48].

2.2. Computational methods and model clusters

Here, we briefly explain computational methods; unrestricted Hartree Fock method (UHF) and hybrid-DFT [49–51] methods (UHF, UB2LYP. UB3LYP and UBLYP). In the hybrid-DFT calculations, exchange-correlation potentials are generally defined by:

$$EX_C = C_1EX_{HF} + C_2EX_{Slater} + C_3EX_{Becke88} + C_4EC_{VWN} + C_5EC_{LYP}, \tag{4}$$

where the third and fourth terms in this equation mean Becke's exchange correlation [52] involving the gradient of the density and Vosko, Wilk and Nusair (VWN) [53] correlation functional, respectively, and the last term is the correlation correction of Lee, Yang and Parr (LYP) [54] which includes the gradient of the density. C_i (i = 1–5) are the mixing coefficients. The parameter sets C_1, C_2, C_3, C_4 and C_5 are 0.5, 0.5, 0.5, 1.0 and 1.0 for UB2LYP, 0.2, 0.8, 0.72, 1.0 and 0.81 for UB3LYP and 0.0, 1.0, 1.0, 1.0 and 1.0 for UBLYP [47–51]. All hybrid density functional (HDFT) calculations were performed by using GAUSSIAN94 program [55] package.

As is well known [4], conventional DFT such as BLYP overestimate metallic character, and copper oxides become metal instead of AF insulator under the DFT approximation. While, the HDFT methods such as UB2LYP have been sucesssfully applied to transition metal oxides such as copper- and nickel oxides [47–50]. First of all, let us consider cluster models (**I**–**V**) in Fig. 2 in order to elucidate the interrelationships among the computational schemes in 2. The dimer model (**I**) for the nearest neighbor pair of **1**–**4** is investigated as the

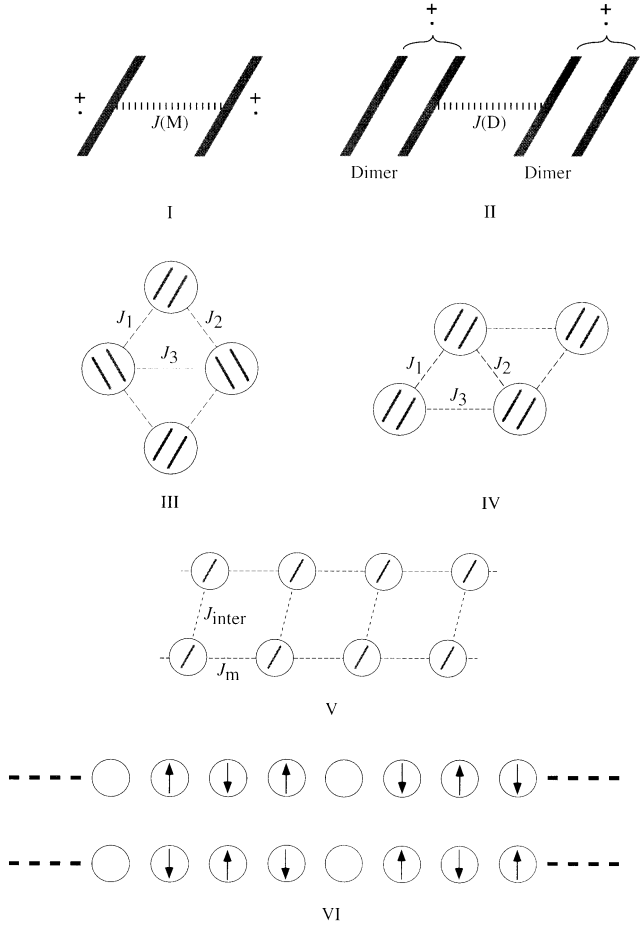

Fig. 2. The effective exchange interaction between dimer dication (**I**) and between dimer of dimer cation (**II**), those of κ-(BETS)$_2$X (**III**) and λ-(BETS)$_2$X (**IV**), and intra- and inter-chain effective exchange interactions in quasi-1D systems (**V**). The stripe structure is illustrated in **VI**.

simplest model for elucidation of characteristics of UHF and HDFT methods.

2.3. Calculated effective exchange integrals

To estimate the magnitude of the magnetic interaction for the nearest neighbour biradical pair (**I**) of BEDT-TTF (**3**) and BETS (**4**) cation radical (half-filling), we have calculated the J_{ab} values. Table 1 summarizes the $J_{ab}^{(1)}(=J_{ab}^{(4)})$, $J_{ab}^{(2)}$ and $J_{ab}^{(3)}$ values for **I** of **3** and **4**, which are estimated by Eqs. (2a), (2b), (2c) and (3). All the calculated J_{ab} values are negative in sign, indicating the AF character. However, the calculated values are considerably different in contrast to those of molecular magnetic materials [20,21]. As for UHF, the differences between $J_{ab}^{(1)}$ and $J_{ab}^{(3)}$ values by our AP procedure were not so large because of strong localization of biradical electrons, while $J_{ab}^{(2)}$ is about one-half of $J_{ab}^{(3)}$ as expected at the strong correlation limit. On the other hand, $J_{ab}^{(1)}$ becomes about twice of $J_{ab}^{(3)}$ under the UBLYP approximation since the UBLYP solution is reduced to the spin-restricted BLYP one (RBLYP). Then, $J_{ab}^{(2)}$ is similar to $J_{ab}^{(3)}$ in this weak correlation limit. The spin projection effect is crucial in this limit, and it is quite significant under the UB2LYP and UB3LYP approximations. These results indicate that radical pair (I) of **3** or **4** belongs to the intermediate orbital interaction region, $|J_{ab}^{(2)}|<|J_{ab}^{(3)}|<|J_{ab}^{(1)}|$, in contrast to the magnetic limit where $|J_{ab}^{(3)}|=|J_{ab}^{(1)}|$ and the nonmagnetic limit where $|J_{ab}^{(3)}|=|J_{ab}^{(2)}|$. Since we can estimate the chemical bonding region of **I** using different computational schemes Eqs. (2a), (2b) and (2c), J_{ab} values can be regarded as the sensitive parameter to diagnose the chemical bonding between HOMO a and HOMO b in **I**.

Since our computational scheme in Eq. (2c) works well in the whole region, namely weak to strong through intermediate correlation regime, our scheme is used for later calculations.

3. Hubbard and $t-J$ models for strong correlation systems

3.1. Model Hamiltonians and electronic properties

In this section, we briefly summarize theoretical background for molecular design of functional materials. Previously, we have examined electronic structures of high-T_c copper oxides using ab initio MO methods [47–51,56], showing the necessity of N-band models for systematic descriptions of magnetism, conductivity and superconductivity of the species as illustrated in Fig. 3. Some organometallic and organic systems isoelectronic to copper oxides have been also proposed on the basis of the ab initio results [5,6]. N-band models often reduce to the two-band model, which has been used for elucidation of Kubo–Inagaki [57,58] mechanism of ferromagnetism (FM) and other magnetic states, and Suhl–Kondo mechanism [59,60] and related multi-band models [61–64] for superconductivity. In previous papers [61–64], the two-band model combined with

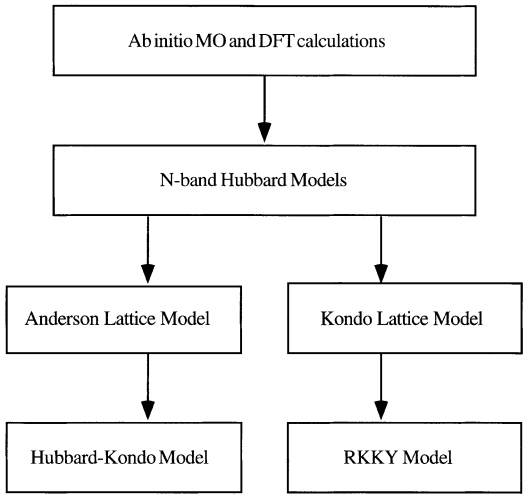

Fig. 3. Ab intio MO and DFT calculations and mutual relations among effective model Hamiltonians.

Table 1
Effective exchange integrals evaluated by several types of Eq. (2) for nearest neighbor donor pair A in κ-phase BETS and BEDT-TTF salts (cm^{-1})

	J_{ab} (1)	$J_{ab}^{(2)}$	$J_{ab}^{(3)}$	$J_{ab}^{(4)}$	$J_{ab}^{(5)}$ [a]
Donor pair A in κ-phase $(BETS)_2FeCl_4$					
UHF/6-31G	−269	−135	−264	−269	−291
UB2LYP	−599	−299	−543	−599	−693
UB3LYP	−1204	−602	−822	−1204	−1335
UBLYP	−2438	−1219	−1218	−2438	−3576
Donor pair A in κ-phase $(BEDT\text{-}TTF)_2FeCl_4$					
UHF/6-31G	−286	−143	−280	−286	−271
UB2LYP	−523	−261	−479	−523	−531
UB3LYP	−950	−475	−693	−950	−995
UBLYP	−2009	−1005	−1004	−2009	−2523

[a] Perturbation calculation (Eq. (10)).

the temperature Green function technique has been applied to elucidate phase diagrams of charge density wave (CDW), SDW, singlet superconductivity (SSC), triplet superconductivity (TSC) and FM. The g-ology for the SSC phase is regarded as an extension of Suhl–Kondo mechanism [59,60] for superconductivity. Instead of the two-band model, Anderson lattice model [65] or Kondo lattice model [66] can be used for theoretical descriptions of ferromagnetic (FM) metals, paramagnetic metals and spin liquid of electron of hole doped conducting polymers interacting with coordination compounds with spins ($M^{\bullet}$) [61,62] and donor (D)–acceptor (A) complexes, where D or A are interacting with the magnetic species ($M^{\bullet}$) [5,63]. The so-called RKKY model [67–69] is used for theoretical description of effective exchange couplings of spins via the spin polarization of conduction electron. The RKKY model has been employed for theoretical studies of FM, AFM, helical spin structure and spin glass of organic and organo-metallic magnetic materials. The Hubbard–Kondo model is also utilized to describe the external magnetic field effects such as Jaccarino–Peter effect [38].

3.2. Hubbard models for p–d, π–d and π–R systems

The ab initio calculations of large magnetic clusters in Section 2 are often time-consuming. Therefore, the extended Hubbard Hamiltonian [5,70,71] can be generally used for p–d, π–d and π–R systems which are insulators because of electron correlation effects

$$H = H_q + H_r + H_{qr} \tag{5}$$

where H_q denotes the Hamiltonian for p(π)- or d-electron, and H_{qr} is the interaction Hamiltonian between them as follows:

$$H_q = \sum T_{qq} a_q^+ a_q + \sum U_{qr} a_q^+ a_q b_r^+ b_r \quad (q, r = \mathrm{p},\ \pi \text{ and } \mathrm{d})$$
$$H_{qr} = \sum T_{qr} (a_q^+ b_r + b_r^+ a_q) \tag{6}$$

where a^+ and b^+ create electron (or hole) on the qth a-site and the rth b-site, respectively. U_{qq} and U_{qr} ($=$V) are on- and inter-site Coulomb repulsions, and T_{qq} ($=\varepsilon_{qq}$) and T_{qr} are orbital energy and transfer integral between p(π)- and d(R)-orbitals, respectively. The parameters used in Eq. (6) were estimated from the ab initio results and spectroscopic data as shown previously [71]. The CT excitation energy (Δ_{qr}) from donor site to the acceptor vacant orbital is given under the Hubbard model as:

$$\Delta_{qr} = (\varepsilon_{rr} - \varepsilon_{qq}) + (U_{rr} - U_{qq}) \tag{7}$$

For example, the transition metal oxides are classified from the relative magnitude of U_{dd} ($r=$d) and Δ_{pd} ($q=$p) into three types: (a) CT insulator ($\Delta_{pd} < U_{dd}$); (b) intermediate case ($\Delta_{pd} = U_{dd}$); and (c) Mott–Hubbard insulator ($\Delta_{pd} > U_{dd}$). In our parametrization [71], Cu and Ni oxides belong to the CT insulator, while Cr, V and Ti oxides such as V_2O_3 and Ti_2O_3 are classified into the Mott–Hubbard insulator. The Co, Fe and Mn oxides are regarded as the intermediate case. The hole is mainly introduced at ligand site in the case of CT insulators, while it lies on metal site for the Mott–Hubbard insulators. The isoelectronic π–d ($r=$d and $q=\pi$) and π–R ($r=$R and $q=\pi$) systems were proposed on the basis of these relationships (a)–(c). Table 2 summarizes p–d, π–d and π–R systems examined previously [14–28].

3.3. Heisenberg model

The Hubbard model often reduces to the Heisenberg spin Hamiltonian in the case of strong electron correlation systems. The exact diagonalization (full CI) of singlet and triplet CI matrices of the Hubbard model provide the effective exchange integral in Eq. (1) as

$$E_{CI}(\text{singlet}) - E_{CI}(\text{triplet}) = 2J_{dd} \tag{8}$$

The Hubbard model often reduces to the Heisenberg spin Hamiltonian in the case of strong electron systems. The exact diagonalization (full CI) of singlet and triplet CI matrices of the Hubbard model provide the effective exchange integral in Eq. (1). If the effective exchange integral (Eq. (8)) between transition metal ions is weak, it can be approximately given by the perturbation theory as:

$$J_{dd} = -\frac{2T_{pd}^4}{\Delta_{pd}}\left\{\frac{1}{\Delta_{pd}^2} + \frac{1}{U_{dd}\Delta_{pd}}\right\} = -2(t_{dd})^2\left\{\frac{1}{\Delta_{pd}} + \frac{1}{U_{dd}}\right\} \tag{9a}$$

$$= \frac{-2(t_{dd})^2}{\Delta_{pd}} \quad (t_{dd} = T_{pd}^2/\Delta_{pd}) \tag{9b}$$

From Eq. (9a), J_{dd} is sensitive to the magnitude of Δ_{pd} and U_{dd}. Its magnitude increases sharply with the decrease of Δ_{pd} as in the case of copper oxide, and it is approximately given by Eq. (9b). On the other hand, J_{dd} in Eq. (9a) is reduced to the following familiar form if $U_{dd} < \Delta_{pd}$: namely the Mott–Hubbard case.

$$J_{dd} = -\frac{2t_{dd}^2}{U_{dd}} \tag{10}$$

The transition metal fluorides [6] usually correspond to this case because the p-level of fluoride anion is deep. As shown later, the Heisenberg model is used for theoretical description of magnetism in many organic charge-transfer (CT) complexes such as κ-(BEDT-TTF)$_2$X. The J_{ab} values for several magnetic systems with and without doping are given in our other papers [45,46].

Table 2
Magnetic conductors and organometallic magnetic conductors

Type	p–d	π–d	π–Ṙ
Intra-molecular	Copper oxides	Conducting polymer with metal complexes	Conducting polymer with organic radicals
Inter-molecular	Metal assembled complexes	TTF-type donors with metal complexes	TTF-type donor with organic radicals
References	[5,6,17,50]	[5,16,25,26]	[14,15,18,20–24,27,28]

Previously, we have estimated the bonding parameters such as transfer integral and on-site repulsion on the basis of the above equations using the J_{ab} values calculated by HDFT methods [45,46]. The perturbation scheme in Eq. (10) was applied to the radical pair (I) of **3** and **4**. The calculated results are given in Table 1. From Table 1, the calculated J_{ab} values by the perturbation method becomes very large in magnitude, showing its breakdown for copper oxide species [5] and other strong electron-correlation systems [45].

4. Theory of superconductivity near AF state

4.1. Superconductivity by t–J model

Previously [61–64], the four-component spinor (Nambu expression) was introduced to characterized possible electronic phase of molecular materials: (1) CDW; (2) SDW; (3) singlet superconductor (SSC); (4) triplet superconductor (TSC); and (5) FM metal. The phase diagrams of these states were depicted using two-band model in combination of the temperature Green function technique (see Fig. 4). Our theoretical investigations elucidated four different approaches to obtain high-T_c superconductors in the intermediate regime of the metal insulator transitions [61]. One of them is an approach from the strong correlation limit using the resonating valence bond (RVB), while spin-fluctuation model from the metallic side is another approach: these were referred to as the unified J-model [5,6] as illustrated in Fig. 4.

Our unified J-model [5,6] was extended so as to reproduce experimental results on the basis of Ginsburg–Landau (GL) model derived from the slave–boson treatment of t–J model [72]. The transition temperatures for AF and SSC phases were given by:

$$T_C(X) \propto \sqrt{J_1 J_2}(x_{min}(X) - x) \quad (X = \text{AF or FM}) \tag{11a}$$

$$T_C(Y) \propto \sqrt{J_1 J_2}(x_{max}(Y) - x)(x - x_{min}(Y)) \quad (X = \text{SSC or TSC}) \tag{11b}$$

$$T_C(Z) \propto \sqrt{J_1 J_2}(x_{max}(Z) - x)(x - x_{min}(Z)) \quad (X = \text{SG}) \tag{11c}$$

where $x_{min}(Z) = x_{min}(X)/x_{max}(Y)$ and x is the hole concentration, and x_{min} and x_{max} are its lower and upper limits for phase transitions X, Y and Z. The T_c for AF or FM phases decreases with the increase of x ($x < x_{min}(X)$), while T_c for SSC or TSC has the maximum in the intermediate region ($x_{min}(Y) < x < x_{max}(Y)$). The states exist under the spin gap (SG) or

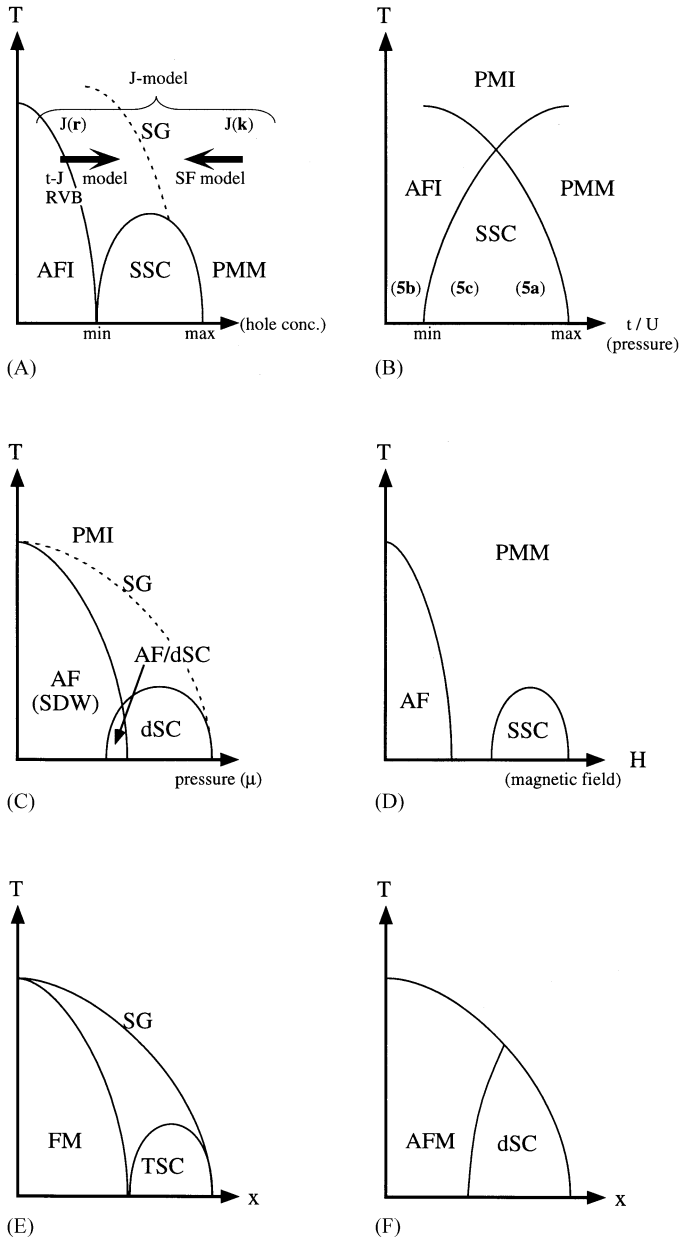

Fig. 4. Several phase diagrams (A)–(F) for molecular materials with strongly correlated electron systems (see text).

pseudo gap phase as illustrated in Fig. 4. The origin of the high-T_c superconductivity of copper oxides is regarded as strong effective exchange interaction ($2|J| > 1000$ cm^{-1}) [6]. This implies that an attractive interaction between holes is J in our J-model [5,6]. This model at least works well for a simple explanation of high-T_c superconductivity of copper oxides, as well as κ-(BEDT-TTF)$_2$X.

In order to confirm the above simple picture, exact diagonalizations [4] of finite clusters have been performed for the Hubbard model. Our J-model [5] is consistent with recent numerical calculations [4] for the two-dimensional (2D) t–J model, which have elucidated relative stabilities among the AF state and several SSC states with different symmetries:

$$\Delta k = \begin{pmatrix} \Delta\text{:s-wave} \\ \Delta \sin k_x \sin k_y\text{:d}_{xy}\text{-wave};\ \ \Delta(\cos k_x - \cos k_y)\text{:d}_{x^2-y^2}\text{-wave} \\ \Delta(\sin k_x + C \sin k_y)\text{:(s + d)-wave} \\ \Delta(\sin k_x + \mathrm{e}^{i\theta} \sin k_y)\text{:(s + id)-wave} \end{pmatrix} \tag{12}$$

where the k-space representation is used instead of the site representation in Eq. (12). The states with $C = 1$ and -1 denote, respectively, the extended s-wave and pure $d_{x^2-y^2}$ (d)-wave and the state with $\theta = \pi/2$ means the (s + id)-state. At the half-filling state (no-hole), the AF state is more stable than the SSC state with the $d_{x^2-y^2}$ symmetry, or d_{xy} symmetry, though the d_{xy} wave is believed to be the most stable for κ-(BEDT-TTF)$_2$X among the SSC states in Eq. (12). On the other hand, the $d_{x^2-y^2}$ wave SSC state becomes the ground state for copper oxides in the approximately hole-doped region, in accord with the experiment [4].

Interestingly, the quantum Monte Carlo calculations [4] have indicated that the kinetic energy (t) does not favor the superconductivity in all the hole-doped region. The exchange term (J) gives the attractive force in the $d_{x^2-y^2}$ channel, supporting our J-model [5,6]. In fact, the energy gap in Eq. (12) is numerically given by $\Delta = 0.15J - 0.27J$ [4] ($= 1.13\ T_c$ by the BCS theory), supporting Eq. (11b). The transition temperature (T_c) can be easily estimated by inserting the ab initio J_{ab} values in this relation, providing that $T_c = 50$–150 K. The estimated values are consistent with the experiments for high-T_c cuprate superconductors [4]. Thus, ab initio J_{ab} calculations followed by the exact diagonalization of Hubbard and t–J models are useful for theoretical studies of superconductivity in strong correlation systems.

4.2. Spin mediated models for superconductivity for 1D and 2D system

Recent experiments [29–31] have demonstrated that AF phase exists near the SC state of the highest T_c organic superconductors; κ-(BEDT-TTF)$_2$X (X = 9Cu(NCN)$_2$ (**5a**), Cu[N(CN)$_2$]Cl (**5b**), Cu[N(CN)$_2$]Br (**5c**)). **5a** and **5c** are superconductors. On the other hand, **5b** is a paramagnetic insulator (PMI), but an antiferromagnetic insulating phase (AFI) is stabilized below $T_N = 27$ K at ambient pressure [29]. With increasing pressure, the Neel temperature of AFI is suppressed and the singlet superconducting phase (SSC) appears. The SSC transition temperature of **5b** takes its maximum value ($T_{SSC} = 13$ K) at 300 bar, but the SSC phase is also suppressed under high pressure, giving rise to paramagnetic metal (PMM) phase. Fig. 4(B) illustrates the phase diagram for **5a**, **5b** and **5c** at ambient pressure [30,31].

The extended Hückel band models usually provide Fermisurfaces for organic charge transfer complexes constructed of BEDT-TTF and their derivatives, and simple band pictures have been used for qualitative explanations of electronic properties of these complexes [39]. However, the Mott–Hubbard transitions often occur in organic charge-transfer complexes such as **5b** and the magnetic properties of these complexes are expressed by the Heisenberg model, where the d–d orbital interaction (t_{dd}) in Eq. (10) and on-site repulsion integral (U_{dd}) are replaced with the π–π interaction ($t_{\pi\pi}$) of the donor molecules and $U_{\pi\pi}$ via sulphur atom contact.

Both ab initio and semiempirical calculations [73,74] have been performed to determine reasonable parameters of the Hubbard models for **5b**. The Hubbard models for **5b** were solved by the mean field approximation to reproduce the experimental phase diagram in Fig. 4(B) [75]. The Hubbard model for **5b** was investigated by the FLEX method, which can treat AFM and superconductivity (SSC) on equal footing, and it was shown that d-wave SSC is realized in a wide region of the phase diagram next to the AF phase [76]. The dynamical susceptibility and self energy (see in Eq. (23) below) for a simplified dimer Hubbard model were calculated by FLEX, and T_{SSC} obtained by solving the

Table 3
Effective exchange integrals between dimer dication of BEDT-TTF (**3**) (cm^{-1})

	J_1	J_2	J_3
5a	−61.0	−61.0	−35.5
5b	−71.6	−71.6	−30.2
5c	−78.7	−78.7	−25.2

linearized Elishberg type equation (see also Eq. (20)) was in good agreement with the experiment [77]. The third-order correction in Eq. (23) was also examined to confirm the spin fluctuation mediated superconductivity for **5b** [78]. The multicritical phenomena of SSC and AF for **5b** was analyzed in terms of the renormalization and SO(5) symmetry groups [10], suggesting that the origin of the SSC with d-wave symmetry is common with that of the AF. All these advanced theories [72–80] indicated an important role of electron correlation (EC) effect for SSC and AF for **5b**.

As shown in **I** of Fig. 2, we have calculated the J_{ab} (M) values between monomer cations (namely one-hole in each monomer (M)) of **5a**, **5b**, **5c** and **5d** (X = Cu[N(CN)$_2$]I) by UB3LYP/6-31G, assuming the X-ray geometries of each dimers. The spin-projected scheme in Eq. (2c) was used for comparison with other groups (see later). The J_{ab} (D) values between dimer cations (namely one-hole in each dimer) (II) in Fig. 2 was simply estimated by assuming J_{ab} (D) = J_{ab} (M)/2. Table 3 summarizes the calculated results. The J_{ab} (M) values for the nearest neighbour pairs were smaller than −500 cm^{-1}, showing the strong HOMO–HOMO interaction. Then the exchange interactions in tetramers with two holes are approximately regarded as those between dimer cations with one hole as illustrated in Fig. 2(B). The calculated J_{ab} (D) values are in the range; −25 − 80 cm^{-1}, being compatible with the experimental values for **5a** and **5b**. Therefore, if we assume the J-model of copper oxides for T_{SSC}, $\Delta = 0.10J - 0.15J$ [4] (= 1.13 T_c by the BCS theory), the estimated T_{SCC} is in the experimental order because $J = 100$ K for **5a** and **5b**. However, the symmetry of d-wave SC, d_{xy} or $d_{x^2-y^2}$ in Eq. (12) was not settled experimentally.

The J_{ab} values (J_m) for the nearest pair (I) for $(TMTSF)_2PF_6$ are about −500 cm^{-1}, while the interchain ones of Fig. 2 are only −18 to −34 cm^{-1} since the interchain distance is large. Therefore, T_c given by Eq. (11b) should be low (about 1 K) because of the weak interchain interaction. This in turn indicates that our J-model based on spin fluctuation or electron correlation works well for organic metals with strong electron correlations.

4.3. SO(5) and QED$_3$ models

Zhang has given a SO(5) model that has unified AFM and singlet dSC [10]. This symmetry enables the construction of SO(5) quantum nonlinear σ model that describes the phase diagram and the effective low-energy dynamics of the system. This model naturally explains the basic phenomenology of the high-T_c superconductivity from the insulating to the underdoped region, where electron correlation effect plays an essential role. The SO(5) theory permits the coexistence of AF and SSC phases as illustrated in Fig. 4(C). Nagao et al. [81] have extended the SO(5) theory to the FM to triplet superconducting state (TSC) and have obtained the phase diagrams for FM state and TSC as illustrated in Fig. 4(E).

In the SO(5) theory, the AF and dSC parameters are unified into a five-dimensional vector (n_i, $i = 1-5$) called a superspin [10,82]. The AF order parameters m correspond to the (n_2, n_3, n_4) components, while the real and imaginary parts of the superconducting order parameter (dSC) ψ correspond to the (n_1, n_5) components.

$$F = \frac{1}{2}\rho\left|\left(\nabla + \frac{ie^*}{\hbar c}A\right)\psi\right|^2 - \frac{1}{2}\chi(2\mu)^2|\psi|^2 + \frac{1}{2}\rho|\nabla m|^2 - \frac{1}{2}gm^2 + \frac{1}{8\pi}(\nabla \times A)^2 \quad (13)$$

The chemical potential (μ) induces a phase transition for AF to dSC. The free energy by the SO(5) theory is given by where $\psi = n_1 + in_5$ and $m = n_2x + n_3y + n_4z$ are the dSC (ψ) and AF (m) order parameters and χ is the susceptibility. When $g_1 = g - 4\mu^2\chi$ is negative, dSC is the ground state, while AF state is preferred when g_1 is positive. The SO(5) theory has been applied to several model Hamiltonians such t–J model and Hubbard model. It has been found that there is a coexistance of dSC and AF in a special case as shown in Fig. 4(E) [11].

Very recently, the (2+1) dimensional quantum electrodynamics (QED$_3$) theory has been proposed as an effective model for description of superconductor–insulator transition and pseudo gap (SG) phase in underdoped cupurates [11,12], where the so-called stripe structure in **VI** of Fig. 2 has been observed. Other phases with broken chiral symmetry are the (d+ip) and (d+is) insulators, and CDW and SDW. The QED$_3$ theory has been extended to magnetic field induced SDW forming in the neighbourhood of a vortex, in agreement with neutron scattering and tunneling spectroscopy experiments [7–9]. Ohsaku et al. [83] have presented a QED theory for magnetic field induced SDW and dSC. The SO(5) and QED$_3$ models have provided the mathematical foundations of our J-model for magnetism and

superconductivity of molecular systems in intermediate or strong correlation regime.

5. Theory of superconductivity related metal

5.1. Gorikov theory for BCS superconductors

The t–J model has been used for theoretical description of underdoped copper oxides and related strong correlation species, which lie near the magnetic insulating state (see Fig. 4). On the other hand, conventional BCS model starts from the metallic state, where phonon and charge fluctuations are employed as attractive interaction for Cooper pair formation. In fact, the phonon mechanism has been proposed for many crystals of TTF derivatives [39]. Therefore, we revisit the Gorikov's

$$H = \sum_{\mathrm{k}\sigma} \varepsilon_{\mathrm{k}} c^{\dagger}_{\mathrm{k}\sigma} c_{\mathrm{k}\sigma} + \sum_{\mathrm{q}} \omega(\mathrm{q}) a^{\dagger}_{\mathrm{q}} a_{\mathrm{q}} + \frac{1}{\sqrt{N}} \sum_{\mathrm{k},\mathrm{q},\sigma} \alpha(\mathrm{q})(a_{\mathrm{q}} + a^{\dagger}_{\mathrm{q}}) c^{\dagger}_{\mathrm{k}+\mathrm{q}\sigma} c_{\mathrm{k}\sigma} \tag{14}$$

approach [84] for BCS superconductor since it can be used to derive the McMillan equation [16] for computation of T_{c}. The e–p interaction (Fröhlich) Hamiltonian [85] is generally given by where $\omega(\mathrm{q})$ and $\alpha(\mathrm{q})$ denote phonon frequency ($\hbar = 1$) and interaction matrix element between electron and phonon. The normal and abnormal Green functions for electrons are introduced for formulation of superconductivity in conformity with Gorikov [84] as

$$G(\mathrm{k},\ \tau - \tau') = -\langle \mathrm{T} c_{\mathrm{k}\uparrow}(\tau) c^{\dagger}_{\mathrm{k}\uparrow}(\tau') \rangle \tag{15a}$$

$$F^{*}(\mathrm{k},\ \tau - \tau') = -\langle \mathrm{T} c^{\dagger}_{-\mathrm{k}\downarrow}(\tau) c^{\dagger}_{\mathrm{k}\uparrow}(\tau') \rangle \tag{15b}$$

where T is the Wick operator which reorders the operators in such a way that τ increases from right to left, and $\langle\ \rangle$ means the thermal average. Similarly, the Green function for phonon is given by:

$$D(\mathrm{q},\ \tau - \tau') = -\langle T \phi_{\mathrm{q}}(\tau) \phi^{\dagger}_{\mathrm{q}}(\tau') \rangle \tag{15c}$$

where

$$\phi_{\mathrm{q}}(\tau) = (a0(\tau) + a_{-\mathrm{q}}(\tau)) \tag{16}$$

In order to evaluate Green functions [61–64], we must solve the equation of motions in the Heisenberg representation. The complicated thermal average of two particle interactions is decoupled under the mean field approximation. The decoupled equations after Fourier transformations are solved by defining normal and abnormal self energies as:

$$\Sigma(\mathrm{k},\ i\varepsilon_n) = -\frac{k_B T}{N} \sum_{q,m} \alpha^2(k-q) \times D(k-q,\ i\varepsilon_n - i\varepsilon_m) G(q,\ i\varepsilon_m) \tag{17}$$

$$\Delta(k,\ i\varepsilon_n) = \frac{k_B T}{N} \sum_{q,m} \alpha^2(k-q) D(k-q,\ i\varepsilon_n - i\varepsilon_m) \times F(q,\ i\varepsilon_m) \tag{18}$$

The equation of motions for Green functions is usually referred to as the Eliashburg equation [86]

$$\begin{pmatrix} i\varepsilon_n - \varepsilon_{\mathrm{k}}(\mathrm{k}) - \Sigma(\mathrm{k},\ i\varepsilon_n) & -\Delta(\mathrm{k},\ i\varepsilon_n) \\ \Delta^{*}(\mathrm{k},\ i\varepsilon_n) & i\varepsilon_n + \varepsilon(\mathrm{k}) + \Sigma(\mathrm{k},\ -i\varepsilon_n) \end{pmatrix} \times \begin{pmatrix} G(\mathrm{k},\ i\varepsilon_n) \\ F^{*}(\mathrm{k},\ i\varepsilon_n) \end{pmatrix} = \begin{pmatrix} 1 \\ 0 \end{pmatrix} \tag{19}$$

The Eliashburg equation involves the normal self energy Σ, in addition to the abnormal one Δ, and the retardation effect for the electron–phonon interaction is taken into account through the Green function for phonon. From Eq. (19), we have the gap equation to determine the transition temperature (T_{c}).

$$\Delta(\mathrm{k},\ i\varepsilon_n) = -\frac{\mathrm{k}_B T}{N} \times \sum_{\mathrm{q},m} \alpha^2(\mathrm{k}-\mathrm{q}) D(\mathrm{k} - \mathrm{q},\ i(\varepsilon_n - \varepsilon_m)) G(\mathrm{q},\ i\varepsilon_n) G(-\mathrm{q}, -i\varepsilon_n) \Delta(\mathrm{q},\ i\varepsilon_m) \tag{20}$$

This is solved in the self consistent manner.

Ignoring the k-dependence of Δ, the gap equation is simplified and, for practical purpose, instead of solving Eq. (19), the McMillan equation [87] can be used to determine T_{c} as:

$$T^{\mathrm{McM}}(a) = \frac{\omega_{\log}}{1.2} \exp\left[\frac{-1.04(1+\lambda)}{\lambda - \mu^{*}(1 + 0.62\lambda)}\right] \tag{21}$$

where μ^{*} is the effective screened Coulomb repulsion, and λ is dimensionless electron–phonon coupling constant given by a complex averaging over a Fermi surface [5]. The band calculations of a lot of organic metals constructed of TTF derivatives have been published on the basis of bonding parameters obtained by the extended Huckel calculations. Mori has summarized available results [39].

5.2. Non BCS mechanism

The charge or spin fluctuation (SF) model [61–64] is often employed to explain the superconductivity of (over) doped copper oxides [4] on the basis of possible electronic mechanism. It was also applied to design isoelectronic organometallic and organic systems [5,6]. In this situation, the electron–phonon interaction part in Eq. (20) is replaced by the effective electron–electron interaction via charge and spin fluctuations under the random phase approximation (RPA).

$$\Delta(\mathrm{k},\ i\varepsilon_m) = -\frac{k_B T}{N}\sum_{\mathrm{q},\mu}\Gamma_{\sigma,-\sigma}(\mathrm{k},\ \mathrm{q},\ i\varepsilon_n,\ i\varepsilon_m)G(\mathrm{q},\ i\varepsilon_m) \times G(-\mathrm{q},\ -i\varepsilon_m)\Delta(\mathrm{q},\ i\varepsilon_m) \tag{22}$$

where

$$\Gamma_{\sigma,-\sigma}(\mathrm{k},\ \mathrm{q},\ i\varepsilon_n,\ i\varepsilon_m) = U - \frac{1}{2}\ U^2\chi_c(\mathrm{k}-\mathrm{q},\ i\varepsilon_n - i\varepsilon_m) + \frac{1}{2}\ U^2\chi_s(\mathrm{k}-\mathrm{q},\ i\varepsilon_n - i\varepsilon_m) + U^2\chi_s(\mathrm{k}+\mathrm{q},\ i\varepsilon_n + i\varepsilon_m) \tag{23}$$

The χ_c and χ_s denote, respectively, dynamic charge and spin susceptibilities given by the corresponding correlation functions. Therefore, the charge fluctuation model [87] is available if χ_c is predominant, while great importance of χ_s is assumed for SF model: note that the third and fourth terms in Eq. (23) are longitudinal and transverse SFs, respectively [61–64]. Thus, our J-model is used in abroad sense to cover SF in the k-space [61–64]. The transition temperature for SSC is expressed by the conventional BCS formula as illustrated in Fig. 4(A) [5]

$$T_c(\mathrm{SSC}) = \Gamma_q\xi_m(x_{\max}-x)(x-x_{\min})\exp\left(-\frac{1}{\lambda}\right) \tag{24}$$

where the cutoff energy is given by the characteristic energy Γ_q of charge or spin fluctuation and ξ_m is the magnetic coherence length [88].

6. Magnetic conductors and superconductors via π–d interactions

6.1. Anderson and Kondo lattice models

As shown in Fig. 2, molecular systems described by multi-band models are our theoretical targets to realize multifunctional materials. Previously, we have used Anderson and Kondo lattice models [5] for molecular design of doped-magnetic polymers and segregated columns of CT complexes coupled with coordination compounds with spins ($M^\bullet$). Very recently, AF and FM metal states were discovered for organic–inorganic hybrid systems as discussed later. The Anderson model Hamiltonian for these species is given by:

$$\begin{aligned} H &= \sum \varepsilon_k c^\dagger_{k\sigma}c_{k\sigma} + \sum E_R M^\dagger_{i\sigma}M_{i\sigma} + U\sum_i M^\dagger_{i\uparrow}M_{i\uparrow}M^\dagger_{i\downarrow}M_{i\downarrow} \\ &\quad + T\sum_{i\sigma}(M^\dagger_{i\sigma}c_{k\sigma} + c^\dagger_{k\sigma}M_{i\sigma}) \\ &= \sum \varepsilon_k c^\dagger_{k\sigma}c_{k\sigma} + \sum E_R M^\dagger_{k\sigma}M_{k\sigma} \\ &\quad + \frac{U}{N_0}\sum_{k,k',q} M^\dagger_{k+q\uparrow}M^\dagger_{k'-q\downarrow}M_{k'\downarrow}M_{k\uparrow} \\ &\quad + T\sum_{k\sigma}(M^\dagger_{k\sigma}c_{k\sigma} + c^\dagger_{k\sigma}M_{k\sigma}) \end{aligned} \tag{27}$$

where ε_k is the energy level of conduction electron and U and E_M denote the on-site Coulomb repulsion of spin site ($M^\bullet$) and SOMO energy level of $M^\bullet$, respectively, and T is the interaction matrix element between conduction and SOMO electrons. The electronic structures of the Anderson lattice model are highly dependent on relative magnitudes of ε_k, E_M and U as discussed previously [56]. The so-called Kondo regime [60] is defined as a specific state where the SOMO level (E_M) is deeper than Fermi level (ε_F), even if the band width (Γ) of radical electrons is taken into account ($\varepsilon_F - E_M \gg \Gamma$), where $E_M + U - \varepsilon_F \gg G$ because of the strong on-site repulsion U of radical sites. This implies that subtle balances of Fermi (HOMO) levels of conducting polymers (or CT complexes) and SOMO levels of coordination compounds, together with Coulomb repulsion (U) for spin sites are necessary for achievements of Kondo regime. In fact, we have examined the energy levels of TTF-spin ($M^\bullet$) systems by the ab initio calculations and have shown that such a situation can be realized in the system [56]. The situation is similar in the case of some TTF-derivatives plus transition metal complexes.

In this situation, spins on the spin sites are alive under chemical and physical dopings in the field effect transistor (FET) configuration to generate conduction electrons [28,45]. Therefore, several spin-mediated electronic states such as FM metal and spin mediated superconductivity are expected in Kondo regime. Slave boson method, which eliminates the double occupancy of radical states (see Refs. [72,80]), can be used to solve the Anderson lattice model [65] to depict the phase diagram. Some SOMO electrons on radical sites are almost localized in the Kondo regime, only their spin freedom remains, leading to the Kondo lattice model as follows:

$$H_{KM} = \sum_{k\sigma}\varepsilon_k c^\dagger_{k\sigma}c_{k\sigma} + J_{CM}\sum \sigma_i\cdot S_i \tag{28}$$

where S_i means spin localized at radical site i and σ_i

denotes the spin of conduction electron.

$$\sigma_i = \frac{1}{2}\sum_{\sigma\sigma'} c^{\dagger}_{i\sigma}\boldsymbol{\tau}_{\sigma\sigma'}c_{i\sigma'} \tag{29}$$

where $\boldsymbol{\tau} = (\tau_x, \tau_y, \tau_z)$ is Pauli spin matrix. The Kondo lattice model has been used for molecular design of organic Kondo and dense Kondo systems, together with π–d conjugated systems [20].

Since localized spin $\langle S_i \rangle$ at site i induces the local magnetic field ($-J_{CM}\langle S_i \rangle$) on conduction electrons, the spin polarization on site j is given by:

$$\langle S^{\alpha}_j \rangle = -J_{CM}\sum_{\beta=x,y,z}\chi^{\alpha\beta}(j,\ i)\langle S^{\beta}_i \rangle \tag{30}$$

where $\chi_{ab}(j, i)$ denotes the local magnetic susceptibility. Then, the magnetic interaction of localized spin $\langle S_j{}^{\alpha} \rangle$ at site j with $\langle S_j{}^{\beta} \rangle$ is defined by:

$$H_{RKKY} = -J^2_{CM}\sum_{\langle ij\rangle}\sum_{\alpha\beta} S^{\alpha}_j\chi^{\alpha\beta}(j,\ i)S^{\beta}_i \tag{31a}$$

$$= -2J_{ij}\sum_{\langle ij\rangle} S_j\cdot S_i \tag{31b}$$

where

$$\frac{1}{2}J^2_{CM}\chi^{\alpha\beta}(j,\ i) = J_{ij}\delta_{\alpha\beta} \tag{32}$$

Thus, the exchange couplings between radical spins via the spin polarization of conduction electrons are described by the RKKY type spin Hamiltonian [67–69]. The RKKY model has been used for molecular design of several magnetic states of magnetic polymers and crystals as shown below.

6.2. Hubbard–Kondo model for magnetic field effect

The magnetic impurities such as Fe(III) ions with $S = 5/2$ classical spin in CuO_2 plane destroy the superconductivity like the external magnetic field [4–6]. Recent discovery of magnetic-field-induced superconductivity in the two-dimensional (2D) compound, λ-$(BETS)_2X$, has therefore provided an interesting theoretical problem [32–34]. Below 8 K, λ-$(BETS)_2X$ is an AF insulator. As a magnetic field is applied, it undergoes a first-order transition to a metal at 11 T. If the magnetic field is parallel to the layers, there is transition to a SC state at 20 T, which is destroyed at 42 T as illustrated in Fig. 4(D). In order to explain these phenomena, Brossard et al. introduced the Hubbard–Kondo model [89] as:

$$H_q = \sum T_{qq}a^{+}_q a_q + \sum U_{qq}n_q(\uparrow)n_q(\downarrow) - J\sum S_i\sigma_i + g_a\mu_B H\sum S^z_i + g_a\mu_B H\sum \sigma^z_i \tag{33}$$

where $n_q(\uparrow)$ denotes the density of up spin at site q, S_i is a spin operator for the local moment, and J is the effective exchange integral between conduction electron and local spin of X ($= FeCl_4$).

Let us consider the two limits of small and large U. For small U, the effective exchange interactions between local spins are given by the above RKKY model given by Eq. (32). For large U, the magnetic interaction energy is given by $-JS/2$ per site since the system is a Mott insulator. If we neglect the fluctuations of the localized spins and consider the regime where the spins are aligned by the magnetic field, the third (Kondo) term in Eq. (33) is replaced with [35–37]

$$J\sum S_i\sigma_i = -JS\sum \sigma^z_i \tag{34}$$

The effective magnetic field experienced by the electrons is given by $H - H_e$, where $H_e = JS/g\mu_B$. At $H = H_e$, the Hamiltonian is the same as for the compound without the magnetic ions (X), for example, λ-$(BETS)_2GaCl_4$, which is a superconductor. This gives $J = -1.6$ meV (-9.2 cm^{-1}) for $H = 33$ T [35].

6.3. Ab initio calculation of Kondo coupling

In order to elucidate the magnitude of effective exchange interaction between conduction electron and localized spins of $Fe(III)Cl_4$, Kawakami et al. [45,56] have carried out the UB3LYP calculations of the Kondo coupling in Eq. (34) in λ-$(BETS)_2FeCl_4$ (**6a**) and κ-$(BETS)_2FeCl_4$ (**6b**). The calculated J values are -9.2, -1.2, -1.2 and -0.0 (cm^{-1}) for near BETS–$FeCl_4$ pairs of **6a**, respectively. Since they have used Eq. (2c), the largest J-value (9.2) is about twice of the experimental one (note $J = 2J_{ab}$ in our definition). On the other hand, the J value was calculated to be about -3.4 cm^{-1} for the nearest BETS–$FeCl_4$ pair of **6b**. Since the optimal magnetic field for **6b** is 12 T, the relative magnitude of the calculated Kondo coupling is parallel to the experiment by Uji et al. [32–34]. Since we have employed the small cluster models, our calculated $|J|$-values should be the maximum limits for **6a** and **6b**. On the other hand, $|J|$-values of the metallic limit by 31 should be the minimum limits for them. Ab initio DFT calculations [56] for J-values of model clusters are useful for qualitative understanding of the Kondo coupling. The details of the computational results are given in the paper by Kawakami et al. in this issue [90].

7. Molecular design of magnetic conductors

We have theoretically examined possible organic, organometallic analogs to copper oxides and magnetic conductors on the basis of both ab initio and Hubbard model calculations as described above. In fact, several strategies are presented: (1) magnetic modification of

TTF derivatives [20]; (2) magnetic modification of conducting polymer [15]; (3) magnetic modification of Ni(dimt) systems [25,26]; and (4) construction of organic RVB [18]. Past decade, experimental results for the first systems (1) have been reported. Then, we wish to discuss these results in relation to our theoretical models proposed previously [5,6].

7.1. Magnetic modifications of organic metals

Previously [5], we have pointed out that TTF-derivatives plus metal complex MX_4 are regarded as π–d conjugated system. Very recently, Kobayashi coworkers [90–95] found that a series of λ- and κ-$(BETS)_2$ MX_4 systems ($MX_4 = GaCl_4$, $FeCl_4$, $FeBr_4$, $(Fe_xGa_{1-x})Cl_4$ and $FeBr_x$ Cl_{1-x}) exhibit the metal–insulator transitions, superconductivity, coexistence of superconductivity and AFM, and other electronic properties. For example, λ-$(BETS)_2GaCl_4$ and λ-$(BETS)_2FeCl_4$ exhibited, respectively, a superconductivity transition at $T_{SSC} = 8$ K, and a coupled metal–insulator and AF transition at 8.5 K. The localized spin of Fe(III) ion ($S_a = 5/2$) clearly suppressed the superconductivity. The hybrid systems, λ-$(BETS)_2$ $(Fe_xGa_{1-x})Cl_4$ and $(BETS)_2FeBr_xCl_{1-x}$ indicated interesting mixed electronic and magnetic properties, which were highly sensitive to the concentration x, external pressure and other structural factors. While, κ-$(BETS)_2FeBr_4$ was an AF organic metal at ambient pressure ($T_N = 2.5$ K), showing the existence of π–d interaction between conduction electron and Fe(III) spin (Fig. 4(F)). Moreover, the heat capacity experiment suggested the coexistence of the superconductivity and AF long-range order below $T_{SSC} = 1$ K. The same situations appeared in the case of κ-$(BETS)_2FeCl_4$, though the corresponding phase transition temperatures became low; $T_N =$ 0.65 K and $T_{SSC} = 0.1$ K, respectively.

Experimentally, the exchange coupling constants between conduction electron and Fe(III) spin are in the range: −8–23 K [90–95]. Judging from T_N for AF order, the magnitude should become large in the case of $FeBr_4$ salts. Thus, the p–d interaction increases in the following order:

$$FeCl_4 \rightarrow FeBr_xCl_{1-x} \rightarrow FeBr_4 \quad (35a)$$

$$\text{BEDT-TTF} \rightarrow \text{BETS}$$

$$\text{(substitution of 4S with 4Se)} \quad (35b)$$

These tendencies are reasonable from the view points of spin delocalization in MX_4 and intermolecular orbital overlap. The calculated Kondo couplings [45,90] J by UB3LYP are consistent with the recent experimental results [90–95].

7.2. Magnetic modifications of conducting polymers

The introduction of spin fluctuation from the metallic side (see Fig. 4(A)) of conducting polymers [17–19] would be a simple analogy to Little's exciton model [96] for the high-T_c superconductor, though the charge fluctuation is replaced by the spin fluctuation. Before the discovery of the cupurate high-T_c superconductor [1],we have interested in hole or electron doping into magnetic polymers to design organic magnetic metals [14,15,27]. Theoretical calculations on model aromatic systems showed that organic polymers; polyphenylene, polyphenylene vinylene, polypyrole so on, could be modified into pendant type magnetic semiconductors or insulators by introducing radical groups as side substituents [5,14,15]. Theoretical possibilities of conversions from these ferro- or ferri-magnetic polymers into magnetic conducting polymers by hole (or electron) doping were also examined by using several aromatic ion radicals with radical substituent [14,15]. The high-spin ground states were often resulted by these computations, and were explained by the double exchange, spin-polarization (SP) and spin-delocalization (SD) mechanisms, leading to a proposal of organic ferro- and/or ferri-magnetic metals in Fig. 5. The spin-mediated superconductor via spin-fluctuation is also

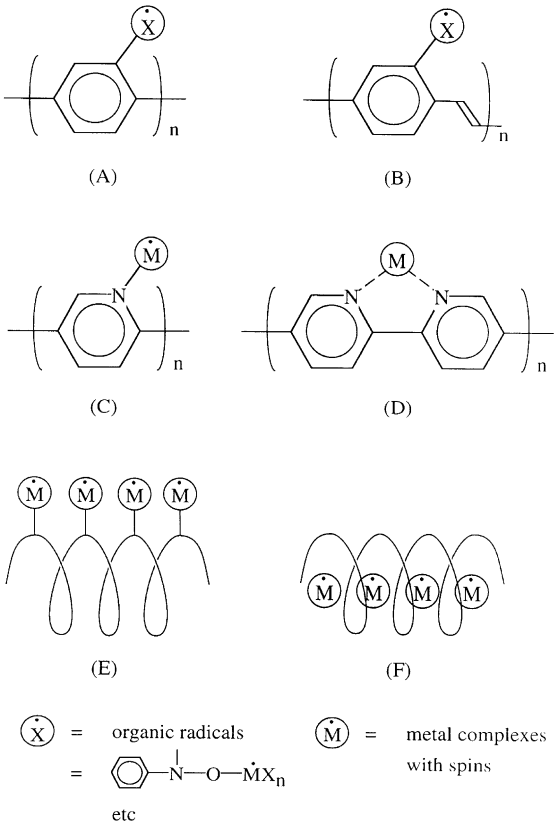

Fig. 5. Possible π–d and π–R systems consisted of conducting polymers and local spins.

conceivable for these metals. Very recently, we made extensive DFT calculations of both oligomers and polymers [27]: the results were consistent with the previous results [17]. However, recent two-band model calculations [81] have indicated that well-organized polymer solids are necessary for realization of long-range magnetic or SC order.

Nishide et al. [97] first synthesized the pendant-type FM oligomers with poly(phenylene vinylene) skeleton by introducing nitroxide, phenoxy radicals as radical sources. Doping of these species would be interesting from the present theoretical model [5]. Recently, Yamamoto et al. [98] synthesized the polymers involving nitrogen atoms within the main chain as illustrated in Fig. 5. The coordination of transition metal complexes with spin(s) to the nitrogen lone pair would provide the π–d systems which are particularly interesting from the molecular magnetism. In fact, these should be well described by the periodic Anderson Hamiltonian, where the π-orbital of poly(pridine) system plays an important role. The doping of hole or electron into π-network may exhibit several exotic phases in Fig. 4, depending on the strength of pπ–dπ interactions [5]. Probably, magnetic modifications of helical conducting polymers are next targets, which would be molecular solenoids as illustrated in Fig. 5.

7.3. Pure organic magnetic conductors

The magnetic modifications of CT complexes by introduction of organic radicals as spin sources [15,19,20] would be a simple analogy to SF model for the high-T_c superconductor [5]. After the discovery of the cuprate high-T_c superconductor [1],we have interested in introduction of stable radical species to CT complexes and organic metals such as TTF-derivatives in Fig. 1. Theoretical calculations on model aromatic systems showed that organic metals such as TTF, DTPY so on [20] could be modified into magnetic conductors by introducing radical groups. The spin-mediated superconductor via spin-fluctuation is also conceivable for these metals because radical species can be taken to be free radical with $S = 1/2$ to enhance spin fluctuation. Very recently, we have made extensive DFT calculations of oligomers of model compounds [99]: the results were consistent with the previous results [20].

Nakasuji et al. [100] have synthesized various CT complexes between electron acceptor (TCNE for example) and TTF derivatives with nitroxide radical group(s). The CT complexes have exhibited the semiconducting properties instead of magnetic metal. Sugawara and coworkers [101] have also synthesized the TTF-derivatives with nitroxide group, and have shown the triplet ground state for the cation diradical. Morita et al. have synthesized the precursor of high-spin ion radicals [102]. Model calculations [99] indicate that active controls of magnitude of effective exchange interactions between conduction electron and spin of radical group is crucial to realize pure magnetic conductors [20].

In conclusion, theoretical backgrounds for molecule-based magnetic conductors are summarized here since many numerical results are given in several papers in this issue [90,99]. Interplay between theory and experiments is very productive in the field of molecule-based materials, showing possibility of synthesis of many interesting pure organic magnetic conductors in future.

Acknowledgements

This work has been supported by Grants-in-Aid for Scientific Research (No. 14204061) from the Ministry of Education, Science, Sports, and Culture, Japan.

References

[1] J.G. Bednort, K.A. Muller, Z. Phys. 64 (1986) 189.
[2] A.P. Kampf, Phys. Reps. 249 (1994) 219.
[3] W. Brenig, Phys. Rep. 251 (1995) 153 (and references therein).
[4] M. Imada, A. Fujimori, Y. Tokura, Rev. Mod. Phys. 70 (1998) 1040.
[5] K. Yamaguchi, Int. J. Quant. Chem. 37 (1990) 167.
[6] K. Yamaguchi, Y. Takahara, T. Fueno, K. Nasu, J. Appl. Phys. 26 (1987) L1362; 26 (1987) L2037; 27 (1987) L509.
[7] S. Katano et al., Phys. Rev. Lett. B62, (2000) 14677 (R).
[8] B. Lake, et al., Science 291 (2001) 1759.
[9] J.E. Hoffmann, et al., Science 295 (2002) 466.
[10] S.-C. Zhang, Science 275 (1997) 1089.
[11] E. Delmer, S. Schadev, Y. Zhang, Phys. Rev. Lett. 87 (2001) 067202.
[12] I.F. Herbut, Phys. Rev. B66 (2002) 094504.
[13] M. Franz, D.E. Sheehy, Z. Tesanovic, Phys. Rev. Lett. 88 (2002) 257005.
[14] K. Yamaguchi, Y. Toyoda, T. Fueno, Kagaku 41 (1986) 585 (in Japanese).
[15] K. Yamaguchi, Y. Toyoda, T. Fueno, Synth. metals 19 (l987) 81, 87.
[16] K. Yamaguchi, Kinozairyo 10 (1990) 23 (in Japanese).
[17] K. Yamaguchi, M. Nakano, T. Fueno, Kagaku 42 (1987) 583 (in Japanese).
[18] K. Yamaguchi, Y. Takahara, T. Fueno, K. Nakasuji, I. Murata, Jpn. J. Appl. Phys. 27 (1988) 766.
[19] K. Yamaguchi, H. Namimoto, T. Fueno, T. Nogami, Y. Shirota, Chem. Phys. Lett. 166 (1990) 408.
[20] K. Yamaguchi, M. Okumura, T. Fueno, K. Nakasuji, Synth. Metals 41–43 (1991) 3631.
[21] K. Yamaguchi, M. Okumura, J. Maki, T. Noro, Chem. Phys. Lett. 207 (1993) 9.
[22] K. Yamaguchi, S. Hayashi, M. Okumura, M. Nakano, W. Mori, Chem. Phys. Lett. 266 (1994) 372.
[23] S. Yamanaka, et al., Chem. Phys. Lett. 233 (1995) 257.
[24] S. Yamanaka, et al., Chem. Phys. Lett. 233 (1995) 88.
[25] M. Fujiwara, T. Matsushita, K. Yamaguchi, T. Fueno, Synth. Metals 41–43 (1996) 3267.
[26] M. Fujiwara, S. Takamizawa, W. Mori, K. Yamaguchi, Mol. Cryst. Liq. Cryst. 279 (1996) 1.
[27] M. Mitani, Y. Takano, Y. Yoshioka, K. Yamaguchi, J. Chem. Phys. 111 (1999) 1309.

[28] F. Matsuoka, et al., Polyhedron 20 (2001) 1169.
[29] K. Miyagawa, A. Kawamoto, Y. Nakazawa, K. Kanoda, Phys. Rev. Lett. 75 (1995) 1174.
[30] K. Kanoda, Physica C 282–287 (1997) 290.
[31] K. Kanoda, Hyperfine Interaction 104 (1997) 235.
[32] S. Uji, et al., Nature 410 (2001) 908.
[33] S. Uji, et al., Phys. Rev. B64 (2001) 024531.
[34] S. Uji, et al., Phys. Rev. B65 (2002) 113101.
[35] L. Balicas, et al., Phys. Rev. Lett. 87 (2001) 067002.
[36] K. Capelle, Phys. Rev. B65, (2002) 100515 (R).
[37] M. Houzet, A. Buzdin, L. Bulaevskii, M. Maley, Phys. Rev. Lett. 88 (2002) 227001.
[38] V. Jaccarino, M. Peter, Phys. Rev. Lett. 9 (1962) 290.
[39] T. Mori, Bull. Chem. Soc. Jpn. 71 (1998) 2509.
[40] A.P. Ginsberg, J. Am. Chem. Soc. 102 (1980) 111.
[41] L. Noodleman, J. Chem. Phys. 74 (1981) 5737.
[42] L. Noodleman, E.R. Davidson, Chem. Phys. 109 (1986) 131.
[43] K. Yamaguchi, Y. Takahara, T. Fueno, in: V.H. Smith et al. (Eds.), Appl. Quantum Chem., D. Reidel, 1986, p. 155.
[44] A. Bencini, F. Totti, C.A. Daul, K. Doclo, P. Fantucci, V. Barone, Inorg. Chem. 36 (1997) 5022.
[45] T. Kawakami, et al., Mol. Phys. 100 (2002) 2641.
[46] T. Kawakami, S. Yamanaka, Y. Takano, Y. Yoshioka, K. Yamaguchi, Bull. Chem. Soc. Jpn. 71 (1998) 2097.
[47] T. Onishi, et al., Mol. Cryst. Liq. Cryst. 343 (2000) 133.
[48] M. Mitani, H. Mori, Y. Takano, D. Yamaki, Y. Yoshioka, K. Yamaguchi, J. Chem. Phys. 113 (2000) 4035 (and references therein).
[49] T. Soda, Y. Kitagawa, T. Onishi, Y. Takano, Y. Shigeta, H. Nagao, Y. Yoshioka, K. Yamaguchi, Chem. Phys. Lett. 319 (2000) 223.
[50] T. Onishi, Y. Takano, Y. Kitagawa, T. Kawakami, Y. Yoshioka, K. Yamaguchi, Polyhedron 20 (2001) 1177.
[51] T. Ohnishi, D. Yaniyaki, K. Yamaguchi, Polyhedron (2003), this issue. X-ref: S0277-5387(03)00153-0.
[52] A.D. Becke, Phys. Rev. A38 (1998) 3098.
[53] S.H. Vosko, L. Wilk, M. Nusair, Can. J. Phys. 58 (1980) 1200.
[54] C. Lee, W. Yang, R.G. Parr, Phys. Rev. B37 (1988) 785.
[55] M.J. Frisch, G.W. Trucks, H.B. Schlegel, P.M.W. Gill, B.G. Johnson, M.A. Robb, J.R. Cheeseman, T.A. Keith, G.A. Petersson, J.A. Montgomery, K. Raghavachari, M.A. Al-Laham, V.G. Zakrzewski, J.V. Oritiz, J.B. Foresman, J. Cioslowski, B.B. Stefanov, A. Nanayakkara, M. Challacombe, C.Y. Peng, P.Y. Ayala, W. Chen, M.W. Wong, J.L. Baker, J.P. Stewart, M. Head-Gordon, C. Gonzalez, J.A. Pople, GAUSSIAN 94, Gaussian, Inc., Pittsburgh PA, 1995.
[56] K. Yamaguchi, Y. Kitagawa, T. Onishi, H. Isobe, T. Kawakami, H. Nagao, S. Takamizawa, Coord. Chem. Rev. 226 (2002) 235.
[57] S. Inagaki, R. Kubo, Intern. J. Magnetism 4 (1973) 139.
[58] S. Inagaki, J. Phys. Soc. Jpn. 39 (1975) 596.
[59] H. Suhl, B.T. Matthias, L.R. Walker, Phys. Rev. Lett. 3 (1959) 552.
[60] J. Kondo, Prog. Theor. Phys. 29 (1963) 1.
[61] H. Nagao, M. Nishino, Y. Yoshioka, K. Yamaguchi, Int. J. Quant. Chem. 65 (1997) 947.
[62] H. Nagao, M. Mitani, M. Nishino, Y. Shigeta, Y. Yoshioka, K. Yamaguchi, Int. J. Quant. Chem. 75 (1999) 549.
[63] H. Nagao, M. Nishino, Y. Shigeta, Y. Yoshioka, K. Yamaguchi, J. Chem. Phys. 113 (2000) 11237.
[64] N. Nagao, Y. Kitagawa, T. Kawakami, T. Yoshimoto, H. Saito, K. Yamaguchi, Int. J. Quant. Chem. 85 (2001) 608.
[65] P.W. Anderson, Phys. Rev. 124 (1961) 41.
[66] J. Kondo, Prog. Theor. Phys. 32 (1964) 37.
[67] M.A. Ruderman, C. Kittel, Phys. Rev. 96 (1954) 99.
[68] T. Kasuya, Prog. Theor. Phys. 16 (1956) 45.
[69] K. Yoshida, Phys. Rev. 106 (1957) 893.
[70] J. Hubbard, Proc. R. Soc. (London) A276 (1963) 238.
[71] K. Yamaguchi, M. Nakano, H. Namimoto, T. Fueno, J. Appl. Phys. 27 (1988) L1835; 27 (1989) L479; 28 (1989) L672.
[72] N. Nagaosa, P.A. Lee, Phys. Rev. 64 (1990) 2450.
[73] Y. Imamura, S. Ten-no, K. Yonemitsu, Y. Tanimura, J. Chem. Phys. 111 (1999) 5986.
[74] A. Fortunelli, A. Painelli, Phys. Rev. B55 (1997) 16088.
[75] E. Demiralp, W.A. Goddard, III, Phys. Rev. B56 (1997) 11907.
[76] H. Kino, H. Fukuyama, J. Phys. Soc. Jpn. 65 (1996) 2158.
[77] H. Kino, H. Kotani, J. Phys. Soc. Jpn. 67 (1998) 3691.
[78] H. Kondo, T. Moriya, J. Phys. Soc. Jpn. 67 (1998) 3695.
[79] T. Judo, S. Koikegami, K. Yamada, J. Phys. Soc. Jpn. 68 (1999) 1331.
[80] P.W. Anderson, The Theory of Superconductivity in the High-Tc Cupurates, Princeton University Press, Princeton, 1997.
[81] H. Nagao, M. Nishino, Y. Shigeta, Y. Yoshioka, K. Yamaguchi, Int. J. Quant. Chem. 80 (2000) 721.
[82] D.P. Arovas, et al., Phys. Rev. Lett. 79 (1997) 2871.
[83] T. Ohsaku et al., to be published.
[84] L.P. Gor'kov, Sov. Phys. JETP (Engl. Transl.) 7 (1958) 505.
[85] H. Frolich, Proc. R. Soc. London Ser. A215 (1952) 291.
[86] G.M. Eliashberg, Sov. Phys. -JETP (Engl. Transl.) 11 (1960) 696.
[87] H. Nagao, M. Masaki, M. Nishino, Y. Shigeta, Y. Yoshioka, K. Yamaguchi, Int. J. Quant. Chem. 70 (1998) 1075.
[88] P. Monthoux, D. Pines, Phys. Rev. B47 (1993) 6069.
[89] L. Brossard, et al., Eur. J. Phys. B1 (1998) 439.
[90] T. Kawakami, S. Nakano, Y. Kihagawa, K. Yamaguchi, Polyhedron (2003), this issue. X-ref: S0277-5387(03)00298-5.
[91] H. Kobayashi, H. Tomita, T. Naito, A. Kobayashi, F. Sakai, T. Watanabe, P. Cassoux, J. Am. Chem. Soc. 118 (1996) 368.
[92] H. Akutsu, K. Kato, E. Ojima, H. Kobayashi, H. Tanaka, A. Kobayashi, Phys. Rev. B58 (1998) 9294.
[93] H. Tanaka, A. Kobayashi, A. Sato, H. Akutsu, H. Kobayashi, J. Am. Chem. Soc. 121 (1999) 760.
[94] A. Sato, et al., Phys. Rev. B61 (2000) 111.
[95] H. Kobayashi, A. Kobayashi, P. Cassoux, Chem. Soc. Rev. 29 (2000) 325.
[96] W.A. Little, Phys. Rev. 134 (1964) 25.
[97] H. Nishide, T. Kaneko, T. Nii, K. Katoh, E. Tsuchida, K. Yamaguchi, J. Am. Chem. Soc. 117 (1995) 548.
[98] T. Yamamoto, T. Matsuzaki, A. Minetomo, Y. Kawazu, O. Ohashi, Bull. Chem. Soc. Jpn. 69 (1996) 3461 (and references therein).
[99] T. Taniguchi, S. Nakano, T. Kawakami, K. Yamaguchi, Polyhedron (2203), this issue. X-ref: S0277-5307(03)00256-0
[100] S. Nakasuji, A. Hirai, J. Yamada, K. Suzuki, T. Enoki, H. Anzai, Mol. Cryst. Liq. Cryst. 306 (1997) 409.
[101] H. Sakurai, A. Izuoka, T. Sugawara, Mol. Cryst. Liq. Cryst. 306 (1997) 414.
[102] Y. Morita, et al., Tetrahedron Lett. 42 (2001) 7991.